https://doi.org/10.5194/bg-2020-178
Preprint. Discussion started: 1 July 2020

Diel and seasonal variability of methane emissions from a shallow and eutrophic pond

Wenli Zhang[1], Shangbin Xiao[2*], Heng Xie[1], Jia Liu[2], Dan Lei[2], Andreas Lorke[3]

1 Hubei International Scientific and Technological Cooperation Center of Ecological Conservation and Management in Three Gorges Area, China Three Gorges University, Yichang, 443002, China;

2 College of Hydraulic & Environmental Engineering, China Three Gorges University, Yichang, 443002, China;

3 Institute for Environmental Sciences, University of Koblenz-Landau, Landau, Germany

Email address for each author listed:

zhangwenli@ctgu.edu.cn; shangbinx@163.com; 1182696787@qq.com; ljia@ctgu.edu.cn; leidan@ctgu.edu.cn; lorke@uni-landau.de;

---

* Corresponding author. e-mail: shangbinx@163.com

https://doi.org/10.5194/bg-2020-178
Preprint. Discussion started: 1 July 2020

Abstract

Ponds play a critical role in biogeochemical carbon cycling and have been identified as hot spots of methane (CH_4) emission. Yet, most existing studies focused on ponds in the boreal zone and current estimates of the relevance of ponds in global CH_4 budgets as well as knowledge of the environmental factors regulating their emissions are poorly constrained. Both nutrient concentration and temperature can potentially alter CH_4 dynamics in shallow ponds, but there are still few investigations into the response of CH_4 emission to nutrient enrichment and rising temperatures. Here we studied the magnitude and regulation of two CH_4 pathways (diffusion and ebullition) from a shallow and eutrophic pond located in the subtropical zone in Central China. Ebullitive fluxes were on average 96.4 mg $CH_4 \cdot m^{-2} \cdot d^{-1}$ and contributed 88.6% to the total (diffusive + ebullition) CH_4 emissions. Daily CH_4 fluxes were related to daily mean water temperature, with ebullition having a stronger temperature dependence than diffusion (Q_{10} of 5.52 vs. 2.05). Relationships between temperature and CH_4 emission were affected by seasonal variation of the concentration of total phosphorus. The temperature dependence of both ebullitive and diffusive fluxes increased with increasing phosphorous concentration. Our study highlights that increasing eutrophication by anthropogenic impacts and climate warming will increase CH_4 emissions from ponds, thus representing a positive feedback mechanism to global warming.

Keywords: Subtropical pond; eutrophication; Diel pattern; Temperature dependence; CH_4 ebullition;

https://doi.org/10.5194/bg-2020-178
Preprint. Discussion started: 1 July 2020

1. Introduction

Methane (CH_4) is an important climate forcing as well as a sensitive indicator of climate change due to its increasing atmospheric concentration and its strong global warming potential, which is 28–36 times higher compared to CO_2 (Houghton et al., 2001; Loulergue et al., 2008). Recent estimates report a 150% increase of atmospheric CH_4 concentration since 1750, which is unprecedented over the last 800,000 years (IPCC, 2014). Therefore, a better understanding of CH_4 sources and sinks is urgently needed.

Freshwater ecosystems are important for the biogeochemical processes involved in the cycling of CH_4 (Kirschke et al., 2013; Davidson et al., 2015). There is increasing evidence that freshwaters are a globally significant source of CH_4 (e.g. Lundin et al., 2013). But global CH_4 estimates of freshwaters are based on upscaling of few measurements and still highly uncertain (Rasilo et al., 2015). And before that, numerous ponds and lakes were often considered as minor emitters and their importance was neglected compared to wetland emissions (Wik et al., 2016b). Even small ponds were excluded from most estimates of global carbon budgets (Hanson et al., 2007). However, existing observations of CH_4 fluxes from lakes and ponds suggest that they are emission hot spots (Bastviken et al., 2011; Natchimuthu et al., 2014; Wik et al., 2016a). Especially the small ponds, comprising the majority of lentic aquatic systems (Downing et al., 2006), tend to have higher dissolved CH_4 concentration than larger lakes (Downing et al., 2008; Holgerson, 2015). Holgerson and Raymond (2016) found that very small ponds accounted for 40.6% of diffusive CH_4 emissions from lakes and ponds globally, due to their shallow depth, high sediment to water volume ratios, and frequent mixing. Wik et al. (2016a) compared CH_4 emissions from water bodies north of 50°N, and found that small ponds are an important source of CH_4 in northern latitudes. Nevertheless, current data on the abundance, size, and rate of carbon emissions of small ponds are scarce, which may lead to considerable bias at the regional and global scale (Hanson et al., 2007). More research on the cycling of the CH_4 in ponds will be beneficial to more accurately quantify carbon fluxes from inland waters (Holgerson and Raymond, 2016).

Several studies have explored the dynamics of CH_4 concentrations and fluxes and have linked them to the pond depth and size, weather variables, organic carbon loading and nutrient status (Hamilton and Kelly, 1994; Kankaala et al., 2013; Xiao et al., 2014; Natchimuthu et al., 2014; Holgerson, 2015; Burger et al., 2016). Yet, some studies often relied on short term (30 min) measurements at monthly intervals and temporal variability was poorly resolved (Peixoto et al., 2015). There is still a lack of robust relationships between pond CH_4 and its potential drivers that could facilitate temporal prediction and spatial extrapolation. In addition, most of the studies on CH_4 fluxes from ponds are from the boreal zone, which limits our understanding of inland water carbon cycling at larger scales.

CH_4 can be emitted from aquatic systems through different pathways, including ebullition (bubble emission from sediments) and diffusion (gas exchange at the air-water interface). Small and shallow ponds are expected to become hot spots of ebullition due to limited stratification, sediment temperature being strongly related to atmospheric temperature, and direct solar warming of the sediments (Aben et al., 2017). However, most studies focused on diffusive fluxes and neglected the large emission component of ebullition (Aben et al., 2017). In fact, eutrophic ponds have greater potential for CH_4 ebullition because they accumulate more organic carbon (Downing et al., 2008; Anderson et al., 2014). Increasing eutrophication of aquatic ecosystems by human activities may eventually promote CH_4 ebullition, and the strongest increase in ebullition can be expected in shallow water bodies (West et al., 2016; Aben et al., 2017).

In addition, carbon dynamics in small ponds may be more sensitive to seasonal variation, such as temperature change (Holgerson, 2015). The proportion of ebullitive and diffusive fluxes to total CH_4 emissions may be disproportionally affected by changes in temperature and the temperature dependence of CH_4 fluxes is different with different degrees of aquatic eutrophication (DelSontro et al., 2016). However, there is still no corresponding model basis to evaluate how the magnitude and relative contributions of CH_4 ebullition and diffusion may respond to climatic and environmental changes, including global warming and cultural eutrophication.

This study analyzes CH_4 emissions from a subtropical, shallow and small eutrophic pond in Central China, measured with floating chambers at high temporal resolution (diel variations). We aim at: 1) quantifying CH_4 emissions including diffusive flux and ebullition, with a particular focus on ebullition and its contribution to total CH_4 fluxes; 2) identifying their main influencing factors; and 3) assessing the temperature dependence of ebullitive and diffusive fluxes with different degrees of aquatic eutrophication.

2. Materials and methods

2.1 Study area and monitoring sites

The study was conducted in a small and shallow pond, which is located on the campus of China Three Gorges University, Yichang city, Hubei province, Central China (111°18′23″E, 30°43′24″N). The region is under a subtropical continental monsoon climate regime. The average depth of the pond is 1.2 m, and its area is approximately 4000 m^2. The pond bottom was solidified with concrete in 2002-2003 and is now covered with about 20 cm of soft sediments. The main sources of water are natural rainfall and drainage water from streets. Twelve monthly field campaigns, resolving diurnal variations respectively, were conducted between 19 January and 29 December, 2016. All measurements were done at the same sampling site, which was located 0.5 m away from the bank where water depth was ~ 0.7 m.

2.2 In situ CH_4 flux measurement

CH_4 flux was measured using a static floating chamber and followed the methods described in Xiao et al. (2014). The chamber was made of a non-transparent, thermally insulated vertical tube with a volume of 43.30 L and a surface area of 0.096 m^2 (diameter and height are 0.35 and 0.45 m respectively). Two fans (12 V, 0.22 A) were fixed in the upper part of the chamber to properly mix the air in the chamber headspace while not disturbing the water surface. The chamber was connected to a CH_4 Analyzer (G2301, Picarro, USA), which was used to monitor the CH_4 concentrations inside the chamber continuously at a frequency of 1 Hz. One buoy was fixed at the lower portion of the chamber, allowing for precise adjustment of the penetration depth of the chamber edge into the water. We used 5 cm penetration depth and only the headspace volume above the water surface was taken into account when calculating the gas flux.

Each field campaign was conducted for 24 hours. A single flux measurement was usually finished within 20 minutes and 48 consecutive measurements were conducted during each field campaign. When there was no or little ebullition, CH_4 concentration in the chamber headspace increased nearly linearly over time and single linear regression was used to estimate the diffusive flux of CH_4 (D_{CH4}, mg $CH_4\cdot m^{-2}\cdot h^{-1}$) (Lambert and Fréchette, 2005). When gas bubbles occurred, the gas concentration in the chamber increased abruptly. Under this situation, the flux due to bubble emission (CH_4 ebullition, B_{CH4}, mg $CH_4\cdot m^{-2}\cdot h^{-1}$) was estimated using the method described in detail by Xiao et al. (2014). Bubbles were not observed in all 48 chamber deployments during the daily campaigns. Thus, the frequency of daily CH_4 bubbling (F_{BCH4}) was estimated as:

$$F_{BCH4} = \frac{Deployments\ with\ Bubbles}{48} \times 100\% \qquad \text{(Eq.1)}$$

The daily total CH_4 flux (T_{CH4}, mg $CH_4\cdot m^{-2}\cdot d^{-1}$) was the sum of daily total D_{CH4} and daily total B_{CH4}.

2.3 Model approach

To describe the temperature dependence of CH_4 fluxes, we used a modified Arrhenius equation (Aben et al., 2017):

$$F_{CH4} = F_{20} \times e^{b\times(T-20)} \qquad \text{(Eq.2)}$$

F_{CH4} is the CH_4 flux at temperature T (°C); F_{20} and b are the empirical coefficients; F_{20} is the CH_4 flux at 20 °C. This model can be reorganized as a Q_{10} relationship with b:

$$b = (\ln Q_{10})/10 \qquad \text{(Eq.3)}$$

Q_{10} corresponds to the proportional change in the process per 10 °C change in temperature.

2.4 Other measurements

Air temperature (Ta, °C), air pressure (Pa, hPa), wind speed (w, m s^{-1}) and water temperatures (Tw, °C), and chlorophyll a concentration ($Chl\text{-}a$, μg L^{-1}) were measured every 20 minutes during all diel field campaigns. Ta, and Pa were measured using a handheld weather meter (YGY-QXY, China). Tw was measured using a multi-parameter probe (Hydrolab DS5, HACH, US). Water samples were collected at the beginning of each field campaign. These samples were used to measure the concentrations of *Chl-a*, total nitrogen (*TN*) and total phosphorus (*TP*). *Chl-a* was determined by using the national standard method (Wang et al., 2002). *TN* and *TP* were analyzed spectrophotometrically with a continuous flow autoanalyzer (Skalar Analytical, B.V., Breda, Netherlands). Wind speed was measured with a portable aero vane at 2 m height.

2.5 Statistical analysis

All data were checked for normality using the Kolmogorov-Smirnov test. Pearson's correlations coefficients and linear regressions were used to study the relationships between CH_4 flux and environmental factors. Stepwise linear regressions were performed for relevant combinations of variables. We further estimated seasonal average of variable and defined December, January and February as winter, March to May as spring, June to August as summer, and September to November as autumn.

3. Results

3.1 Variations in environmental factors

Diel and seasonal variations in environmental parameters are summarized in Fig.1. Wind speed was too low to be measured during most campaigns (maximum wind speed was < 1.5 m s^{-1}) and disregarded from further analysis. Air temperature (*Ta*) and water temperature (*Tw*) had significant diel and seasonal changes. The diurnal variation of *Ta* (Δ *Ta*) was greater than that of *Tw* (Δ *Tw*) (Table 1). The maximum Δ *Ta* (27.5°C) and Δ *Tw* (10.1°C) occurred on 28 February and the minimum Δ *Ta* (3.4°C) and Δ *Tw* (1.3°C) occurred on 20 November. The maximum daily mean air temperature ($\overline{Ta}$) was 29.6°C and was recorded on 17 July, and the minimum value was 5.5°C and was measured on 19 January. The extremes in the daily mean water temperatures ($\overline{Tw}$), 30.5 and 8.6°C, were recorded on 29 August and 19 January (Table 1). There were significant seasonal changes of air pressure (*Pa*) and chlorophyll a (*Chl-a*) (Fig 1). The diurnal variation of air pressure (Δ *Pa*) was small. The maximum Δ *Pa* occurred in 29 December and the minimum in 27 October. The maximum daily mean air pressure ($\overline{Pa}$) was recorded on 29 December, and the minimum value was measured on 17 July. Both diurnal and seasonal variations of chlorophyll a (*Chl-a*) ranged widely (Table 1). The maximum diurnal variations of *Chl-a* occurred in 26 April and the minimum in 29 December. The maximum and the minimum daily mean chlorophyll a ($\overline{Chl\text{-}a}$) were recorded on 29 June and 20 November, respectively (27.6 μg L^{-1} to 477.7 μg L^{-1}). With *TN* and *TP* ranging from 1.36 mg·L^{-1} to 5.3 mg·L^{-1} and 0.04 mg·L^{-1} to 0.86 mg·L^{-1}, respectively, the pond can be classified as eutrophic. Both nutrient concentrations were highest in September (Table 1).

We averaged environmental factors in the different seasons and found that *Ta*, *Tw* and *Chl-a* were the highest in summer and the lowest in winter, while *Pa* was the highest in winter and the lowest in summer. There were no significant differences in *Ta*, *Tw*, *Pa* and *Chl-a* between spring and autumn. *TN* and *TP* were highest in autumn and lowest in winter (supplemental Table 1).

3.2 CH_4 fluxes

Diffusive CH_4 fluxes

The diffusive flux of CH_4 (D_{CH4}) from the pond showed obvious but irregular diurnal and seasonal variations (Fig 1). The maximum daily mean diffusive flux ($\overline{D_{CH4}}$) was 0.207 ± 0.009 mg $CH_4 \cdot m^{-2} \cdot h^{-1}$ (mean ± standard error), observed on 18 May. The minimum $\overline{D_{CH4}}$ (0.011 ±

0.001 mg $CH_4 \cdot m^{-2} \cdot h^{-1}$) was on 20 November. D_{CH4} was highest in spring (0.146 ± 0.005 mg $CH_4 \cdot m^{-2} \cdot h^{-1}$) and lowest in winter (0.103 ± 0.006 mg $CH_4 \cdot m^{-2} \cdot h^{-1}$). D_{CH4} in summer was higher than that in autumn. On average, the daily diffusive CH_4 flux of the pond in 2016 was 2.4 ± 0.5 mg $CH_4 \cdot m^{-2} \cdot d^{-1}$ (Table 2).

The highest diel variability in D_{CH4} (Δ D_{CH4}) was observed on 28 February, ranged from 0.083 to 0.455 mg $CH_4 \cdot m^{-2} \cdot h^{-1}$. The lowest ΔD_{CH4} was observed on 20 November, ranged from 0.005 to 0.022 mg $CH_4 \cdot m^{-2} \cdot h^{-1}$. The peak value in 24 h was different during each diel field campaigns. Most of the highest fluxes were observed in the middle of the day or afternoon, when temperatures were higher, such as on 28 February, when D_{CH4} peaked at 16:00 h. Some of the daily maxima occurred when temperatures began to rise rapidly, such as on 16 July, when D_{CH4} peaked at 8:30 h. Accordingly, most of the lowest diffusive fluxed occurred at night or early in the morning, when temperatures were lowest or temperatures began to decrease (Fig 1).

CH_4 ebullition fluxes

Ebullition mainly occurred from May to September, when CH_4 bubbling was not only more frequent (F_{BCH4} exceeding 70%) but also more abundant (Fig 1). Variations of CH_4 ebullition were rather random and irregular. Most of the maximum CH_4 ebullition fluxes (B_{CH4}) during the daily campaign occurred between 0:00 h and 4:00 h, when temperatures were decreasing (such as on 28 February). Some of the maximum B_{CH4} were observed in the afternoon (between 15:00 h and 16:00 h), when temperatures were higher (such as on 17 July), while the maximum B_{CH4} were observed in the morning (about at 6:00 h), when temperatures were lower during other sampling campaigns (such as on 26 April). The relative frequency of occurrence of CH_4

https://doi.org/10.5194/bg-2020-178
Preprint. Discussion started: 1 July 2020

bubbling during the diurnal sampling campaigns (F_{BCH4}) ranged from 4.2% (observed on 19 January and 20 November) to 97.9% (observed on 29 June) (Table 2). Daily total CH_4 ebullition fluxes ranged from 0.3 (on November 20) to 319.9 (on June 29) mg $CH_4 \cdot m^{-2} \cdot d^{-1}$. On average, the daily total CH_4 ebullition flux in 2016 was 96.4 ± 30.5 mg $CH_4 \cdot m^{-2} \cdot d^{-1}$.

The total daily CH_4 flux ($T_{CH4} = D_{CH4+} B_{CH4}$) ranged from 0.5 (on 20 November) to 322.7 (on 29 June) mg $CH_4 \cdot m^{-2} \cdot d^{-1}$, and the mean daily T_{CH4} was 98.7 ± 30.7 mg $CH_4 \cdot m^{-2} \cdot d^{-1}$ (Table 2). The contribution of ebullition (B_{CH4}) to the total flux ranged from 51.8% (on 20 November) to 99.1% (on 29 June). The average daily total CH_4 bubble emissions accounted for 88.6% of the total CH_4 flux (Table 2).

3.3 CH_4 fluxes and environmental factors

Correlation analysis was conducted for D_{CH4} and B_{CH4} obtained from individual chamber deployments, and environmental variables sampled at sub-daily resolution (Table 3). D_{CH4} was positively correlated ($p < 0.01$) with *Tw*, *Ta* and *Chl-a*, while negatively ($p < 0.01$) correlated with *Pa* and the temperature difference between water and air ($\Delta T = Tw - Ta$). B_{CH4} was positively correlated with *Tw*, *Ta* and *Chl-a*, and negatively correlated with *Pa*, but not significantly correlated with ΔT ($p = 0.372$). There was a significant positive correlation between D_{CH4} and B_{CH4} ($p < 0.01$). We explored potential drivers of D_{CH4} and B_{CH4} using stepwise linear regressions (Table 4 and 5). *Ta* could explain most variations in D_{CH4} ($r^2 = 0.25$, $p < 0.001$) and the best multiple regression model included *Ta*, *Pa*, and B_{CH4}, which increased the r^2 to 0.28 ($p < 0.001$). *Tw* could explain most variations in B_{CH4} ($r^2 = 0.14$, $p < 0.001$) and the best multiple regression model included *Tw*, *Chl-a*, and ΔT ($r^2 = 0.20$, $p < 0.001$).

Correlations between CH_4 fluxes and environmental factors in different seasons were analyzed (Table 3, 4 and 5). The result showed that *Tw* was the main factor determining CH_4 fluxes of the pond in autumn, while *Chl-a* was the main factor in summer. Moreover, the main factors determining CH_4 fluxes varied slightly according to CH_4 emission pathway in different season. For diffusion, *Ta* was the main factor in winter; while *Tw* and *Chl-a* were the main factors in spring. For ebullition, *Chl-a* was the main but not strong factor in winter; while the ΔT and *Ta* were the main factors in spring.

We additionally analyzed the relationships between daily total diffusive CH_4 flux (T_{DCH4}), daily total CH_4 ebullition (T_{BCH4}), the frequency of daily CH_4 bubbling (F_{BCH4}) and daily mean values of environmental factors (Table 6). Daily T_{BCH4} and F_{BCH4} were positively correlated with each other and both were positively correlated with $\overline{Tw}$, $\overline{Ta}$ and $\overline{Chl\text{-}a}$, while negatively correlated with $\overline{Pa}$. Daily T_{DCH4} was marginal positively correlated with $\overline{Tw}$, $\overline{Ta}$, T_{BCH4} and F_{BCH4}, while negatively correlated with $\overline{Pa}$. Through stepwise regression, we only obtained a model for daily T_{BCH4}: $T_{BCH4} = -110.47 + 10.17\ \overline{Tw}$ ($r^2 = 0.49$, $p = 0.011$).

The magnitude of the diurnal variation of diffusive CH_4 fluxes (ΔD_{CH4} is difference between maximum flux and minimum flux), daily total B_{CH4}, the frequency of daily CH_4 bubbling (F_{BCH4}) was analyzed with respected to the diel variation of measured parameters (see supplemental Table 2). These analyses showed that ΔD_{CH4} was positively correlated with ΔTw and ΔTa. Through stepwise regression, the best multiple regression model for ΔD_{CH4} was obtained: $\Delta D_{CH4} = 0.01 + 0.036\ \Delta Tw$ ($r^2 = 0.63$, $p < 0.001$). F_{BCH4} was positively correlated with ΔD_{CH4}, and daily total B_{CH4} was positively correlated with F_{BCH4}. Although daily total B_{CH4} was not significantly correlated with ΔTw, we found larger ebullition rates for larger ΔTw for conditions with nearly equal water temperature. For example, the daily mean *Tw* on 28

February (16.1ºC) was close to that on 25 March (16.3ºC), yet Δ *Tw* on 28 February was much higher (10.1ºC) than that on 25 March (2.8ºC). As a result, daily amount of CH_4 ebullition on 28 February (T_{BCH4}, 52.0 mg $CH_4 \cdot m^{-2} \cdot d^{-1}$) was obviously higher than that on 25 March (18.3 mg $CH_4 \cdot m^{-2} \cdot d^{-1}$). This phenomenon was also seen on 29 December and 19 January (Table 1and 2).

3.4 Influence of temperature on diffusion and ebullition

We bin-averaged gas fluxes according to the temperature difference between the surface water and air ($\Delta T = Tw - Ta$) (Fig 2). The results showed that under $\Delta T < 0$ ºC, there was a significant negative linear relationship between D_{CH4} and ΔT ($R^2 = 0.70$). While ΔT was positive but smaller than 5 ºC, D_{CH4} increased slowly. When ΔT was exceeding 5 ºC, D_{CH4} decreased. Besides, when ΔT was nearly zero ($-1 < \Delta T < 1$ ºC), the averaged diffusive CH_4 fluxes (0.091 ± 0.011 mg $CH_4 \cdot m^{-2} \cdot h^{-1}$) was not significantly different from the mean diffusive CH_4 flux for the entire year (0.098 ± 0.019 mg $CH_4 \cdot m^{-2} \cdot h^{-1}$). We also compared the averaged diffusive CH_4 fluxes under $-1 < \Delta T < 1$ ºC with daily mean diffusive CH_4 flux each month (See supplemental Table 3), and found that there were no significant differences between them except for 29 August.

CH_4 ebullition (B_{CH4}) and the frequency of CH_4 bubbling (F_{BCH4}) under different ΔT showed that when ΔT was near zero ($-1 < \Delta T < 1$ ºC), F_{BCH4} was about 30%, and ebullition ranged between 117 ~ 136 mg $CH_4 \cdot m^{-2} \cdot d^{-1}$, which was close to the average CH_4 ebullition flux (96.4 ± 30.5 mg $CH_4 \cdot m^{-2} \cdot d^{-1}$). When $\Delta T > 1$ ºC and $\Delta T < -1$ ºC, F_{BCH4} started to increase. Meanwhile the ebullition flux increased substantially when $1 < \Delta T < 5$ ºC and $-3 < \Delta T < -1$ ºC; yet when $\Delta T > 5$ ºC and $\Delta T < -3$ ºC, the bubbling flux decreased sharply (Fig. 3).

https://doi.org/10.5194/bg-2020-178
Preprint. Discussion started: 1 July 2020

3.5 Temperature dependency of CH_4 fluxes

Temperature was the strongest predictor for seasonal variations of D_{CH4} and B_{CH4}. We calculated the temperature dependence of CH_4 fluxes in terms of Q_{10} (Fig 4). The results showed that the Q_{10} of daily total D_{CH4} of $\overline{Tw}$ and $\overline{Ta}$ were 2.05 and 1.87, respectively. While the Q_{10} of daily total B_{CH4} of $\overline{Tw}$ and $\overline{Ta}$ were 5.52 and 4.38, respectively.

We further explored Q_{10} of ebullition and diffusive emissions for a range of *TP* concentrations (Table 7). Both ebullition and diffusion responded slightly stronger to *Tw* than to *Ta* regardless of *TP* concentrations. For diffusion, Q_{10} increased with *TP* concentration when the averaged *TP* was below 0.4 mg·L^{-1}. For example, when the averaged *TP* was 0.05 mg·L^{-1}, the Q_{10} of the diffusive CH_4 flux for *Tw* and *Ta* were 1.29 and 1.27, respectively. When the averaged *TP* was 0.4 mg·L^{-1}, the Q_{10} of the diffusive CH_4 flux to Tw and Ta increased to 7.52 and 5.23, respectively. However, when averaged *TP* was higher than 0.8 mg·L^{-1}, its Q_{10} tended to decline. For ebullition, although there was no exponential relationship when *TP* was 0.2 ~ 0.4 mg·L^{-1}, Q_{10} also tended to increase with *TP* concentration. For example, when averaged *TP* was 0.05 mg·L^{-1}, Q_{10} of CH_4 ebullition flux to *Tw* and *Ta* were 1.32 and 1.15, respectively. When averaged *TP* was exceeding 0.8 mg·L^{-1}, Q_{10} increased to 3.29 and 2.06, respectively.

4. Discussion

4.1 Contribution of diffusion and ebullition to total CH_4 emissions

The diffusive CH_4 fluxes from the studied pond were on average 2.36 ± 0.07 mg CH_4·m^{-2}·d^{-1}, which is close to the mean diffusive CH_4 fluxes of ponds and small lakes with sizes between 0.1 and 1 km^2 (2.56 mg CH_4 m^{-2}·d^{-1}, Holgerson and Raymond, 2016). However, the diffusive CH_4 fluxes were lower than what has been reported. The diffusive fluxes from a shallow eutrophic lake in southern Brazil, estimated from summer and winter, were 9.35 and 2.17 mg CH_4 $m^{-2}\cdot d^{-1}$, respectively (Palma-Silva et al., 2013). The mean diffusive flux from a tropical pond in India was 49.6 mg CH_4 $m^{-2}\cdot d^{-1}$ (the high diffusive flux from one pond was 324.8 mg CH_4 $m^{-2}\cdot d^{-1}$) (Panneer Selvam et al., 2014). DelSontro et al. (2016) found an average diffusive CH_4 flux of 57.6 mg CH_4 $m^{-2}\cdot d^{-1}$ (from May to November) from ten shallow and vegetated beaver ponds in Canada, which was more than one order of magnitude higher than the diffusive fluxes observed in the present study.

CH_4 ebullition fluxes both in summer and winter in the study (See supplemental Table 1) ranged within the bubble CH_4 emissions reported by PalmaSilva et al. (2013) from a shallow eutrophic lake in southern Brazil. The average CH_4 ebullition flux in our study was 96.4 ± 30.5 mg $CH_4\cdot m^{-2}\cdot d^{-1}$, comparable to the mean ebullition flux from the tropical region in India (112 mg m^{-2} d^{-1}) (Panneer Selvam et al., 2014), while obviously higher than the fluxes reported from lakes in northern Sweden (22.0 mg $CH_4\cdot m^{-2}\cdot d^{-1}$) (Wik et al., 2013), shallow beaver ponds in Canada (73.6 mg $CH_4\cdot m^{-2}\cdot d^{-1}$) (DelSontro et al., 2016), and eight small thaw ponds in northern Sweden (20.0 mg $CH_4\cdot m^{-2}\cdot d^{-1}$) (Burke et al., 2019), all of which are located at high latitudes.

The mean total CH_4 flux of the pond (T_{CH4}) during the whole field investigations was 98.7 [0.5 – 322.7] ± 30.7 mg$\cdot CH_4\cdot m^{-2}$ d^{-1} (mean [range] ± SD, Table 2), which was lower than the ponds (286.4 [3.2 – 833.6] mg$\cdot CH_4\cdot m^{-2}$ d^{-1}), and higher than the lakes (64 [0.32 – 284.8] mg$\cdot CH_4\cdot m^{-2}$ d^{-1}) from the tropical region in India (Panneer Selvam et al., 2014) and from a small shallow pond in Sweden (128 [52.8 – 241.6] mg$\cdot CH_4\cdot m^{-2}$ d^{-1}) (Natchimuthu et al., 2014). A growing body of research has found that ebullition contributed largely to the total CH_4 emissions, such as on average 91 % of the total CH_4 emissions from a small pond in Sweden (its average depth was 1.2 m) (Natchimuthu et al., 2014), 56% from the beaver ponds in Canada (DelSontro et al., 2016), 75% from forty-five aquatic systems in the tropical region of India (Panneer Selvam et al., 2014), and 40–60 % in lakes (Bastviken et al., 2004). In our study, the average contributions of CH_4 ebullition to the total CH_4 flux was at the higher range of observations (88.6%), indicating that ebullition played a major role in CH_4 emissions from the shallow pond studied here. The result confirms that ebullition is an important pathway for CH_4 transport to the atmosphere in shallow aquatic systems, such as ponds (Casper et al., 2000; DelSontro et al., 2016). The larger importance of ebullition in shallow water can be related to the low hydrostatic pressure in the sediment (Bastviken et al., 2004), which reduces the dissolved gas concentration that is required for bubble formation.

Eutrophication could be a contributing factor in the relatively high contribution of ebullition to overall CH_4 flux in our study. The pond studied here was highly eutrophic, with *TP*, *TN* and *Chl-a* exceeding those observed for the beaver ponds in Canada (DelSontro et al., 2016). Eutrophic systems tend to accumulate more organic carbon (Anderson et al., 2014). When substrate is not limiting, there is a greater potential for CH_4 ebullition, thus leading to higher total CH_4 emissions as bubbles directly transport CH_4 to the atmosphere with limited exposure to oxidation (DelSontro et al., 2010).

4.2 Influence of temperature on CH_4 flux

Many studies, including field measurements, indicated that temperature affects CH_4 emissions (Duc et al., 2010; Xing et al., 2005; Natchimuthu et al., 2014; Wik et al., 2014; Aben et al., 2017). In our case, both diffusive and ebullition CH_4 fluxes were positively correlated with *Tw* and *Ta*. For example, variations in *Tw* explained as much as 71 % of the variation in diffusion and 33 % of the variation in ebullition in autumn and variations in *Ta* explained 54 % of the variation in diffusion in winter. Besides, diurnal variation of *Tw* (Δ *Tw*) explained 63 % of the variation of the diurnal pattern of diffusive CH_4 emissions (ΔD_{CH4}). Altogether, our findings confirm that temperature is among the strongest predictors for CH_4 emissions. Methanogenesis is highly temperature dependent (Zimov et al., 1997; Van Hulzen et al., 1999), and higher temperature results in higher CH_4 production rates. In our study, the correlation between *Tw* and diffusive CH_4 flux was almost as strong that with *Ta*. Yet, ebullition was more strongly correlated with *Tw* than *Ta* (Table 3 and Table 6), variations in daily $\overline{Tw}$ explained 49 % of the variation in daily total CH_4 ebullition ($p = 0.011$). Wik et al. (2014) determined sediment temperature to be a significant driver of ebullitive CH_4 flux from shallow lakes. Although the temperature of sediment was not measured in our study, it was mainly controlled by water temperature. For shallow ponds, CH_4 is mainly formed in anoxic sediments, and sediment temperature is likely to increase with air and water temperature. CH_4 emissions may increase with increasing temperature due to the direct temperature effect on methanogenesis in shallow sediments (Bastviken et al., 2008). In addition, ebullition dominated the CH_4 emission in our pond, which might be another reason that CH_4 flux depends on the temperature. Because ebullition largely escapes methane oxidation in the system, it is more directly related to methane production rates in sediments than diffusive emissions (Natchimuthu et al., 2014; Wilkinson et al., 2015). Thus, ebullition responds more directly to Tw because of the stimulatory effects of high temperature on methanogenesis without the confounding effect of methane oxidation.

Convective mixing during nighttime cooling of the water column has been found to coincide with pulses of CH_4 emissions in wetlands (Poindexter, 2016). When the difference between water and air temperature was positive, the diffusive gas fluxed can be expected to be enhanced by high gas exchange velocities (MacIntyre et al., 2001). In our study, when $0 < \Delta T < 5$ ºC, the diffusive CH_4 flux increased slowly, but CH_4 ebullition increased substantially, indicating that the CH_4 flux might be strongly enhanced due to thermal convection. However, when ΔT was exceeding 5 ºC, both diffusion and ebullition tended to decrease. That time was mainly concentrated in the early morning, the temperature was usually the lowest, and lower CH_4 flux was mainly limited by low temperature. When $\Delta T < -3$ ºC, the bubbling flux decreased sharply, while diffusive CH_4 flux increased linearly, indicating that diffusion was an important pathway for CH_4 transport to the atmosphere when the weather was sunny, and air temperature increased more quickly than water temperature. Furthermore, when air temperature was close to water temperature, diffusive fluxes and ebullition were close to their long-term mean values.

4.3 Effects of eutrophication on temperature dependence of CH_4 fluxes

We calculated the temperature dependence of CH_4 fluxes in terms of the temperature coefficient Q_{10}, which was defined by DelSontro et al. (2016) as an "ecosystem-level" Q_{10}, representing the combining effects of multiple biotic and abiotic factors. Q_{10} values in beaver ponds varied slightly according to CH_4 emission pathway and bubbling appeared to be more sensitive to temperature than the diffusive pathway (DelSontro et al., 2016). In our study, the Q_{10} of CH_4 diffusion in respect to $\overline{Tw}$ and $\overline{Ta}$ were 2.05 and 1.87, respectively; while the Q_{10} of CH_4 ebullition of $\overline{Tw}$ and $\overline{Ta}$ were 5.52 and 4.38, respectively. Our values were comparable to those estimated for subtropical and temperate eutrophic city ponds (Q_{10} ranged from1.63 ~ 6.73) (Aben et al., 2017). In contrast to the beaver ponds in Canada, whose average

Q_{10} values for ebullition and diffusion fluxes to sediment temperature were 13 and 10, respectively (DelSontro et al., 2016), our Q_{10} values were lower. Our study also showed that there was a higher temperature sensitivity of bubbling from the ponds, compared to diffusive fluxes. The reason could be due to its very shallow nature and shallow sediment layer, which could cause frequent ebullition and thus promote a more erratic ebullition versus temperature pattern (Wik et al., 2018).

The strong temperature dependence of CH_4 fluxes in our study might be related to its higher productivity. High nutrient concentration promotes the productivity and algal growth (West et al., 2012). The study from the beaver ponds in Canada showed that the temperature dependence of CH_4 fluxes increased with *TP*, and the temperature dependence of ebullition was disproportionately enhanced by ecosystem productivity relative to diffusion (DelSontro et al., 2016). The authors pointed out that as system productivity and the supply of organic matter increased, the CH_4 production was increasingly regulated by temperature (DelSontro et al., 2016). A mesocosm-based study in shallow aquatic systems revealed synergistic effect from combination of nutrient enrichment and experimental warming, causing an increasing mean annual ebullition rate; while the diffusive flux remained unaffected by nutrient enrichment but had a largely positive response to temperature treatment (Davidson, 2018). In our case, Q_{10} of both ebullitive and diffusive fluxes increased with system *TP* within a certain *TP* range. However, the temperature dependence of diffusive fluxes was more sensitive to ecosystem productivity when compared to ebullition. A likely reason for this may be the low frequency of bubbles, which needs more work to be verified.

5. Conclusions

The subtropical, shallow, small and eutrophic pond emitted on average 98.7 ± 30.7 $mg \cdot m^{-2} \cdot d^{-1}$ of CH_4. Ebullition was quantitatively most important, accounting for 51.8% to 99.1% of the total CH_4 emission. A positive correlation between temperature and CH_4 fluxes shows that there are likely positive feedbacks of aquatic CH_4 fluxes to global warming. The temperature dependence of the CH_4 fluxes increased with increasing nutrient concentration. By combing these facts, we conclude that the increasing cultural eutrophication and global warming promote increasing atmospheric CH_4 emissions from these vastly abundant aquatic ecosystems.

6. Data availability

The data published in this contribution can be accessed by email request to the corresponding author.

7. Author contribution

In this work, W.L.Z analyzed the data and wrote the article, S.B.X designed the experiment, H.X, J.L and D.L performed the experiment, and A.L revised the article.

8. Competing interests

The authors declare that they have no conflict of interest.

Acknowledgements

This work was financially supported by the National Science Foundation of China (No. 41273110), Natural Science Foundation of Hubei Province, China (2014CFB672), and Hubei Provincial Department of Education Scientific research projects (Q20151209). The Hubei province Chutian Scholar program (granted to AL) provided additionally financial support for this study. We thank Li Long and Junwei Zhang for their help with fieldwork.

References

Aben, R. C. H., Barros, N., Donk, E. V., Frenken, T., Hilt, S., Kazanjian, G., Lamers, L. P. M., Peeters, E. T. H. M., Roelofs, J. G. M., Domis, L. N. d. S., Stephan, S., Velthuis, M., Van de Waal, D. B., Wik, M., Thornton B. F., Wilkinson, J., DelSontro, T., and Kosten, S.: Cross continental increase in methane ebullition under climate change., Nature communications, 8, https://doi.org/ 10.1038/s41467-017-01535-y, 2017.

Anderson, N. J., Bennion, H., and Lotter, A. F.: Lake eutrophication and its implications for organic carbon sequestration in Europe, Glob Chang Biol, 20, 2741-2751, https://doi.org/ 10.1111/gcb.12584, 2014.

Bastviken, D., Cole, J., Pace, M., and Tranvik, L.: Methane emissions from lakes: Dependence of lake characteristics, two regional assessments, and a global estimate, Global Biogeochemical Cycles, 18, https://doi.org/ 10.1029/2004GB002238, 2004.

Bastviken, D., Cole, J. J., Pace, M. L., and Van de Bogert, M. C.: Fates of methane from different lake habitats: Connecting whole-lake budgets and CH_4 emissions, Journal of Geophysical Research, 113, https://doi.org/ 10.1029/2007JG000608, 2008.

Bastviken, D., Tranvik, L. J., Downing, J. A., Crill, P. M., and Enrich-Prast, A.: Freshwater Methane Emissions Offset the Continental Carbon Sink, Science, 331, 50-50, https://doi.org/ 10.1126/science.1196808, 2011.

Burger, M., Berger, S., Spangenberg, I., and Blodau, C.: Summer fluxes of methane and carbon dioxide from a pond and floating mat in a continental Canadian peatland, Biogeosciences, 13, 3777–3791. https://doi.org/ 10.5194/bg-13-3777-2016, 2016.

Burke, S. A., Wik, M., Lang, A., Contosta, A. R., Palace, M., Crill, P. M., and Varner, R. K.:

Long‐Term Measurements of Methane Ebullition From Thaw Ponds, Journal of Geophysical Research: Biogeosciences, 124, 14, https://doi.org/ 10.1029/2018jg004786, 2019.

Casper, P., Maberly, S. C., Hall, G. H., and Finlay, P. J.: Fluxes of methane and carbon dioxide from a small productive lake to the atmosphere, Biogeochemistry, 49, 1-19, https://doi.org/ 10.2307/1469408, 2000.

Davidson, T. A., Audet, J., Svenning, J.-C., Lauridsen, T. L., Søndergaard, M., Landkildehus, F., Larsen, S. E., and Jeppesen, E.: Eutrophication effects on greenhouse gas fluxes from shallow-lake mesocosms override those of climate warming, Global Change Biology, 21, https://doi.org/10.1111/gcb.13062, 2015.

Davidson, T. A., Audet J., Jeppesen E., Landkildehus F., Lauridsen T. L., Søndergaard M. and Syväranta J.: Synergy between nutrients and warming enhances methane ebullition from experimental lakes, Nature Climate Change, 8, 5, https://doi.org/10.1038/s41558-017-0063-z, 2018.

DelSontro, T., McGinnis, D. F., Sobek, S., Ostrovsky, I., and Wehrli, B.: Extreme Methane Emissions from a Swiss Hydropower Reservoir: Contribution from Bubbling Sediments, Environmental Science & Technology, 44, 2419-2425, https://doi.org/10.1021/es9031369, 2010.

DelSontro, T., Boutet, L., St-Pierre, A., del Giorgio, P. A., and Prairie, Y. T.: Methane ebullition and diffusion from northern ponds and lakes regulated by the interaction between temperature and system productivity, Limnology and Oceanography, 61, S62-S77, https://doi.org/ 10.1002/lno.10335, 2016.

Downing, J. A., Prairie, Y. T., Cole, J. J., Duarte, C. M., Tranvik, L. J., Striegl, R. G., McDowell, W. H., Kortelainen, P., Caraco, N. F., Melack, J. M., and Middelburg, J. J.: The global abundance and size distribution of lakes, ponds, and impoundments, Limnology and Oceanography Methods, 51, 2388-2397, https://doi.org/10.4319/lo.2006.51.5.2388, 2006.

Downing, J. A., Cole, J. J., Middelburg, J. J., Striegl, R. G., Duarte, C. M., Kortelainen, P., Prairie, Y. T., and Laube, K. A.: Sediment organic carbon burial in agriculturally eutrophic impoundments over the last century, Global Biogeochemical Cycles, 22, https://doi.org/10.1029/2006gb002854, 2008.

Duc, N., Crill, P., and Bastviken, D.: Implications of temperature and sediment characteristics on methane formation and oxidation in lake sediments, Biogeochemistry, 100, 185-196, https://doi.org/10.1007/sl0533-010-9415-8, 2010.

Hamilton, J. D., and Kelly, C. A.: Flux to the atmosphere of CH_4 and from wetland ponds on the Hudson Bay lowlands (HBLs), Journal of geophysical research, 99, 16, https://doi.org/10.1029_93JD03020, 1994.

Hanson, P. C., Carpenter, S. R., A., C. J., and Winslow, L. A.: Small lakes dominate a random sample of regional lake characteristics, Freshwater Biology, 52, 9, https://doi.org/10.1111/j.1365-2427.2007.01730.x., 2007.

Holgerson, M. A.: Drivers of carbon dioxide and methane supersaturation in small, temporary ponds, Biogeochemistry, 124, 305-318, https://doi.org/ 10.1007/s10533-015-0099-y, 2015.

Holgerson, M. A., and Raymond, P. A.: Large contribution to inland water CO_2 and CH_4

emissions from very small ponds, Nature Geoscience, 9, 222-226, https://doi.org/10.1038/ngeo2654, 2016.

Houghton, J. T., Ding, Y., Griggs, D. J., Noguer, M., van der Linden, P. J., Dai, X., Maskell, K., and Johnson, C. A.: IPCC 2001, Climate Change 2001: The Scientific Basis, University Press Cambridge, 2001.

IPCC: Climate Change 2014: Synthesis Report. Contribution of Working Groups I, II and III to the Fifth Assessment Report of the Intergovernmental Panel on Climate Change [Core Writing Team, R.K. Pachauri and L.A. Meyer (eds.)]. IPCC, 151, 2014.

Kankaala, P., Huotari, J., Tulonen, T., and Ojala, A.: Lake-size dependent physical forcing drives carbon dioxide and methane effluxes from lakes in a boreal landscape, Limnology and Oceanography, 58, 1915–1930, https://doi.org/ 10.4319/lo.2013.58.6.1915, 2013.

Kirschke, S., Bousquet, P., Ciais, P., Saunois, M., Canadell, J. G., Dlugokencky, E. J., Bergamaschi, P., Bergmann, D., Blake, D. R., Bruhwiler, L., Cameron-Smith, P., Castaldi, S., Chevallier, F., Feng, L., Fraser, A., Heimann, M., Hodson, E. L., Houweling, S., Josse, B., Fraser, P. J., Krummel, P. B., Lamarque, J.-F., Langenfelds, R. L., Le Quéré, C., Naik, V., O'Doherty, S., Palmer, P. I., Pison, I., Plummer, D., Poulter, B., Prinn, R. G., Rigby, M., Ringeval, B., Santini, M., Schmidt, M., Shindell, D. T., Simpson, I. J., Spahni, R., Steele, L. P., Strode, S. A., Sudo, K., Szopa, S., van der Werf, G. R., Voulgarakis, A., van Weele, M., Weiss, R. F., Williams, J. E., and Zeng, G.: Three decades of global methane sources and sinks, Nature geoscience, 6, 813–823, https://doi.org/ 10.1038/NGEO1955, 2013.

Lambert, M., and Fréchette, J.: Analytical techniques for measuring fluxes of CO_2 and CH_4 from hydroelectric reservoirs and natural water bodies, in: Greenhouse Gas Emissions—Fluxes and Processes: Hydroelectric Reservoirs and Natural Environments, edited by: Tremblay, A., Varfalvy, L., Roehm, C., and Garneau, M., Springer, Berlin, 37-60, 2005.

Loulergue, L., Schilt, A., Spahni, R., Masson-Delmotte, V. r., Blunier, T., Lemieux, B. n. d., Barnola, J.-M., Raynaud, D., Stocker, T. F., and Chappellaz, J. r. m.: Orbital and millennial-scale features of atmospheric CH_4 over the past 800,000 years, Nature letters, 453, 383–386, https://doi.org/10.1038/nature06950, 2008.

Lundin, E. J. , Giesler, R. , Persson, A. , Thompson, M. S. , and Karlsson, J. : Integrating carbon emissions from lakes and streams in a subarctic catchment. Journal of Geophysical Research: Biogeoences, 118, 3, https://doi.org/10.1002/jgrg.20092, 2013.

MacIntyre, S., Eugster, W., and Kling, G. W.: The critical importance of buoyancy flux for gas flux across the air-water interface, AGU Geophysical Monograph, 127, 5, 135–139, https://doi.org/10.1029/GM127p0135, 2001.

Natchimuthu, S., Panneer Selvam, B., and Bastviken, D.: Influence of weather variables on methane and carbon dioxide flux from a shallow pond, Biogeochemistry, 119, 403-413, https://doi.org/10.1007/s10533-014-9976-z, 2014.

Palma-Silva, C., Marinho, C. C., Albertoni, E. F., Giacomini, I. B., Figueiredo Barros, M. P., Furlanetto, L. M., Trindade, C. R. T., and Esteves, F. d. A.: Methane emissions in two small shallow neotropical lakes: The role of temperature and trophic level, Atmospheric Environment, 81, 373-379, http://dx.doi.org/ 10.1016/j.atmosenv.2013.09.029, 2013.

Panneer Selvam, B., Natchimuthu, S., Arunachalam, L., and Bastviken, D.: Methane and carbon dioxide emissions from inland waters in India – implications for large scale greenhouse gas balances, Global Change Biology, 20, 3397-3407, https://doi.org/10.1111/gcb.12575, 2014.

Peixoto, R. B., Machado-Silva, F., Marotta, H., Enrich-Prast, A., and Bastviken, D.: Spatial versus day-to-day within lake variability in tropical floodplain lake CH_4 emissions—developing optimized approaches to representative flux measurements, PLoS One, 10, https://doi.org/10.1371/journal.pone.0123319., 2015.

Poindexter, C. M., D. D. Baldocchi, J. H. Matthes, S. H. Knox, and E. A. Variano.: The contribution of an overlooked transport process to a wetland's methane emissions, Geophys. Res. Lett., 43, 9, https://doi.org/10.1002/2016GL068782, 2016.

Rasilo, T., Prairie, Y. T., and Del Giorgio, P. A.: Large-scale patterns in summer diffusive CH_4 fluxes across boreal lakes, and contribution to diffusive C emissions, Global Change Biology, 21, 16, https://doi.org/10.1111/gcb.12741, 2015.

Van Hulzen, J. B., Segers, R., van Bodegom, P. M., and Leffelaar, P. A.: Temperature effects on soil methane production: an explanation for observed variability, Soil Biology & biochemistry, 31, 1919–1929. https://doi.org/10.1016/s0038-0717(99)00109-1, 1999.

Wang, X. F., Wei, F. S., and Qi, W. Q.: Monitoring and Analysis Methods of Water and Wastewater (the fourth edtion). China Environmental Science Press, Beijing (in Chinese), 2002.

West, W. E., Coloso, J. J., and Jones, S. E.: Effects of algal and terrestrial carbon on methane production rates and methanogen community structure in a temperate lake sediment, Freshwater Biology, 57, 949-955, https://doi.org/10.1111/j.1365-2427.2012.02755.x, 2012.

West, W. E., Creamer, K. P., and Jones, S. E.: Productivity and depth regulate lake contributions to atmospheric methane, Limnology and Oceanography, 61, S51-S61, https://doi.org/10.1002/lno.10247, 2016.

Wik, M., Crill, P. M., Varner, R. K., and Bastviken, D.: Multiyear measurements of ebullitive methane flux from three subarctic lakes, Journal of Geophysical Research: Biogeosciences, 118, 1307-1321, https://doi.org/10.1002/jgrg.20103, 2013.

Wik, M., Thornton, B. F., Bastviken, D., MacIntyre, S., Varner, R. K., and Crill, P. M.: Energy input is primary controller of methane bubbling in subarctic lakes, Geophysical Research Letters, 41, 555-560, https://doi.org/ 10.1002/2013gl058510, 2014.

Wik, M., Thornton, B. F., Bastviken, D., Uhlbäck, J., and Crill, P. M.: Biased sampling of methane release from northern lakes: A problem for extrapolation, Geophysical Research Letters, 43, 7, https://doi.org/10.1002/2015GL066501, 2016a.

Wik, M., Varner, R. K., Anthony, K. W., MacIntyre, S., and Bastviken, D.: Climate-sensitive northern lakes and ponds are critical components of methane release, Nature geoscience 9, 7, https://doi.org/10.1038/NGEO2578, 2016b.

Wik, M., Johnson, J. E., Crill, P. M., DeStasio, J. P., Erickson, L., Halloran, M. J., Fahnestock, M. F., Crawford, M. K., Phillips, S. C., and Varner, R. K.: Sediment Characteristics and Methane Ebullition in Three Subarctic Lakes, Journal of Geophysical Research: Biogeosciences, 123, 2399-2411, https://doi.org/10.1029/2017jg004298, 2018.

Wilkinson, J., Maeck, A., Alshboul, Z., and Lorke, A.: Continuous Seasonal River Ebullition

Measurements Linked to Sediment Methane Formation, Environmental Science & Technology, 49, 13121-13129, https://doi.org/ 10.1021/acs.est.5b01525, 2015.

Xiao, S., Yang, H., Liu, D., Zhang, C., Lei, D., Wang, Y., Peng, F., Li, Y., Wang, C., Li, X., Wu, G., and Liu, L.: Gas transfer velocities of methane and carbon dioxide in a subtropical shallow pond, Tellus B: Chemical and Physical Meteorology, 66, 23795, https://doi.org/10.3402/tellusb.v66.23795, 2014.

Xing, Y., Xie, P., Yang, H., Ni, L., Wang, Y., and Rong, K.: Methane and carbon dioxide fluxes from a shallow hypereutrophic subtropical Lake in China, Atmospheric Environment, 39, 5532-5540, https://doi.org/10.1016/j.atmosenv.2005.06.010, 2005.

Zimov, S. A., Voropaev, Y. V., Semiletov, I. P., Davidov, S. P., Prosiannikov, S. F., Chapin, I. F. S., Chapin, M. C., Trumbore, S., and Tyler, S.: North Siberian Lakes: a methane source fueled by Pleistocene carbon, Sciences, 227, 800-802, https://www.jstor.org/stable/2893123, 1997.

Table 1 Daily averaged and diurnal variation of physical and chemical characteristics for each sampling date. Daily mean air temperature ($\overline{Ta}$), daily mean water temperatures ($\overline{Tw}$), daily mean air pressure ($\overline{Pa}$), daily mean chlorophyll a ($\overline{Chl\text{-}a}$), diurnal variation of Ta (ΔTa), diurnal variation of Tw (ΔTw), diurnal variation of air pressure (ΔPa), diurnal variation of chlorophyll a ($\Delta Chl\text{-}a$), daily mean total nitrogen ($\overline{TN}$) and daily mean total phosphorus ($\overline{TP}$).

Note: TN and TP were invalid on 29 December.

Date	$\overline{Ta}$ (°C)	$\overline{Tw}$ (°C)	$\overline{Pa}$ (hPa)	$\overline{Chl\text{-}a}$ ($\mu g\ L^{-1}$)	ΔTa (°C)	ΔTw (°C)	ΔPa (hPa)	$\Delta Chl\text{-}a$ ($\mu g\ L^{-1}$)	$\overline{TP}$ ($mg\ L^{-1}$)	$\overline{TN}$ ($mg\ L^{-1}$)
Jan 19	5.5	8.6	1019	181.3	4.8	1.3	5.1	143	0.04	2.13
Feb 28	15.8	16.1	1013	96.9	27.5	10.1	6.9	81	0.04	2.13
Mar 25	12.8	16.3	1020	180.6	15.0	2.8	4.3	134	0.13	2.98
Apr 26	19.3	21.2	1003	311.6	6.1	2.2	3.0	1091	0.22	2.49
May 18	22.7	24.8	1003	256.7	12.9	3.8	3.5	564	0.33	3.34
Jun 29	24.9	26.5	998	477.7	10.1	3.8	3.1	663	0.10	2.81
Jul 17	29.6	29.4	995	211.2	9.5	5.7	4.0	366	0.07	1.36
Aug 29	25.8	30.5	1003	181.1	15.0	7.4	3.9	341	0.34	3.39
Sep 24	26.3	26.2	1003	420.6	9.7	3.3	3.5	567	0.86	5.30
Oct 27	15.6	17.8	1010	261.5	4.3	1.6	2.9	261	0.86	5.30
Nov 20	16.2	16.9	1009	27.6	3.4	1.3	6.4	76	0.56	4.09
Dec 29	5.7	9.5	1024	53.9	14.6	4.2	9.4	61	----	----

Table 2 Daily total diffusive CH_4 flux (T_{DCH4}), diel variability in D_{CH4} (ΔD_{CH4}), frequency of daily CH_4 bubbling (F_{BCH4}), daily total CH_4 ebullition flux (T_{BCH4}), and daily total CH_4 flux (T_{CH4}) for all sampling campaigns. Bold letters indicated larger ebullition rates for larger ΔTw for conditions with nearly equal water temperature.

Date	ΔD_{CH4} ($mg \cdot m^{-2} \cdot d^{-1}$)	T_{DCH4} ($mg \cdot m^{-2} \cdot d^{-1}$)	F_{BCH4} (%)	T_{BCH4} ($mg \cdot m^{-2} \cdot d^{-1}$)	T_{CH4} ($mg \cdot m^{-2} \cdot d^{-1}$)	T_{BCH4}/T_{CH4} (%)
Dec 29	0.03	0.5	39.6	43.6	44.2	98.8
Jan 19	0.07	1.8	4.2	3.8	5.6	67.8
Feb 28	0.37	4.1	45.8	52.0	56.1	92.6
Mar 25	0.09	1.5	12.5	18.3	19.8	92.4
Apr 26	0.12	2.8	10.4	6.8	9.6	71.1
May 18	0.33	5.0	89.6	235.2	240.2	97.9
Jun 29	0.17	2.7	97.9	319.9	322.7	99.1
Jul 17	0.18	3.2	72.9	134.5	137.8	97.6
Aug 29	0.27	4.2	70.8	149.4	156.7	97.2
Sep 24	0.15	1.7	93.8	174.5	176.3	99.0
Oct 27	0.02	0.4	27.1	17.9	18.3	97.8
Nov 20	0.02	0.3	4.2	0.3	0.5	51.8
All	0.2	2.4±0.5	47.4	96.4 ± 30.5	98.7 ± 30.7	88.6

Table 3 Correlations coefficients among diffusive (D_{CH4}, mg·m^{-2}·d^{-1}) and ebullition (B_{CH4}, mg·m^{-2}·d^{-1}) fluxes observed during individual chamber deployments (576 deployments in total) and environmental variables these variables (water temperatures (Tw, °C), air temperature (Ta, °C), chlorophyll a concentration ($Chl\text{-}a$, μg L^{-1}), air pressure (Pa, hPa), the temperature difference between water and air ($\Delta T = Tw - Ta$, °C)). Correlations are presented for all data and grouped by season.

	CH_4 flux	Tw	Ta	Chl-a	Pa	ΔT	B_{CH4}
All data	D_{CH4}	0.492**	0.499**	0.114**	−0.242**	−0.199**	0.224**
	B_{CH4}	0.372**	0.294**	0.350**	−0.118**	0.042	
Spring	D_{CH4}	0.679**	0.584**	0.171*	−0.640**	−0.161	0.413**
	B_{CH4}	0.400**	0.223**	0.125	−0.269**	0.104	
Summer	D_{CH4}	0.379 **	0.319**	−0.446**	−0.246**	−0.053	−0.199*
	B_{CH4}	−0.194*	−0.258**	0.356**	0.078	0.104	
Autumn	D_{CH4}	0.844**	0.818**	0.662**	−0.760**	−0.412**	0.527**
	B_{CH4}	0.577**	0.558**	0.463**	−0.507**	−0.276**	
Winter	D_{CH4}	0.726**	0.733**	0.024	−0.725**	−0.591**	0.007
	B_{CH4}	0.133	0.243**	−0.011	−0.141	−0.133	

**denotes a significant correlation at the 0.01 level; * denotes a significant correlation at the 0.05 level

Table 4 Stepwise regressions between diffusive flux of CH_4 (D_{CH4}, mg·m^{-2}·d^{-1}), and CH_4 ebullition fluxes (B_{CH4}, mg·m^{-2}·d^{-1}), air temperature (*Ta*, °C), water temperature (*Tw*, °C), the temperature difference between water and air ($\Delta T = Tw - Ta$, °C), air pressure (*Pa*, hPa) and chlorophyll a concentration (*Chl-a*, μg L^{-1}).

Dependent variable	Independent variable	Intercept	Slope	r^2	p
All data					
D_{CH4}	Ta	0.02	0.004	0.25	<0.001
	Ta + Pa	0.07	0.004 − 0.00005	0.27	<0.001
	Ta + Pa + B_{CH4}	0.07	0.004 − 0.00005 + 0.001	0.28	<0.001
Spring					
D_{CH4}	Pa	7.81	− 0.008	0.28	<0.001
	Pa + Chl-a	6.87	− 0.007 + 0.000	0.43	<0.001
	Pa + Chl-a + Tw	−2.17	0.002 + 0.000 + 0.019	0.52	<0.001
	Chl-a + Tw	−2.45	0.000 + 0.016	0.52	<0.001
Summer					
D_{CH4}	Chl-a	0.18	0.000	0.20	<0.001
	Chl-a + Tw	0.08	−0.0001 + 0.003	0.23	<0.001
Autumn					
D_{CH4}	Tw	−0.10	0.007	0.71	<0.001
Winter					
D_{CH4}	Ta	0.02	0.007	0.54	<0.001
	Ta + Pa	6.05	0.004 − 0.006	0.63	<0.001
	Ta + Pa + B_{CH4}	6.21	0.004 − 0.006 − 0.003	0.64	<0.001
	Ta + Pa+ B_{CH4} + Chl-a	7.58	0.004 − 0.007 − 0.003 + 0.000	0.65	<0.001

Table 5 Stepwise regressions between CH_4 ebullition fluxes (B_{CH4}, mg·m^{-2}·d^{-1}) and diffusive flux of CH_4 (D_{CH4}, mg·m^{-2}·d^{-1}), air temperature (Ta, °C), water temperature (Tw, °C), the temperature difference between water and air ($\Delta T = Tw - Ta$, °C), air pressure (Pa, hPa) and chlorophyll a concentration (Chl-a, μg L^{-1}).

Dependent variable	Independent variable	Intercept	Slope	r^2	p
All data					
B_{CH4}	Tw	−3.80	0.39	0.14	<0.001
	Tw + chl-a	−4.28	0.292 + 0.011	0.19	<0.001
	Tw + chl-a + ΔT	−4.99	0.315 + 0.010 + 0.188	0.20	<0.001
	Tw + chl-a+ ΔT+ D_{CH4}	−5.04	0.271+ 0.010 + 0.206 + 8.687	0.20	<0.001
Spring					
B_{CH4}	D_{CH4}	−1.62	40.67	0.17	<0.001
	D_{CH4} + ΔT	−2.98	43.45 + 0.411	0.20	<0.001
	D_{CH4} + ΔT +Ta	−16.29	15.78 + 1.406 + 0.787	0.26	<0.001
	ΔT + Ta	−19.56	1.695 + 1.038	0.25	0.027
	ΔT +Ta +Pa	−502.71	2.74 + 1.998 + 0.459	0.32	0.013
Summer					
B_{CH4}	Chl-a	2.59	0.02	0.13	<0.001
Autumn					
B_{CH4}	Tw	−13.73	0.807	0.33	<0.001
Winter					
B_{CH4}	Chl-a	2.53	− 0.01	0.04	0.015

Table 6 Correlation coefficients between daily total diffusive CH_4 flux (T_{DCH4}, $mg \cdot m^{-2} \cdot d^{-1}$), daily total CH_4 ebullition (T_{BCH4}, $mg \cdot m^{-2} \cdot d^{-1}$), the frequency of daily CH_4 ebullition (F_{BCH4}, %) and mean daily environmental variables (Daily mean air temperature ($\overline{Ta}$, °C), daily mean water temperatures ($\overline{Tw}$, °C), daily mean air pressure ($\overline{Pa}$, hPa), daily mean chlorophyll a ($\overline{Chl\text{-}a}$, $\mu g\ L^{-1}$), daily mean concentrations of total nitrogen ($\overline{TN}$, $mg\ L^{-1}$) and daily mean concentrations of total phosphorus ($\overline{TP}$, $mg\ L^{-1}$)).

Variable	$\overline{Tw}$	$\overline{Ta}$	$\overline{chl\text{-}a}$	$\overline{Pa}$	$\overline{TN}$	$\overline{TP}$	F_{BCH4}	T_{BCH4}
T_{DCH4}	0.568	0.537	0.208	− 0.510	− 0.499	− 0.494	0.551	0.538
	(0.054)	(0.072)	(0.517)	(0.091)	(0.118)	(0.123)	(0.063)	(0.071)
T_{BCH4}	0.703**	0.684**	0.660*	− 0.650*	0.008	− 0.054	0.932**	
	(0.011)	(0.014)	(0.02)	(0.022)	(0.982)	(0.874)	(0.000)	
F_{BCH4}	0.738**	0.735**	0.579**	− 0.635*	0.086	0.083		
	(0.006)	(0.007)	(0.048)	(0.026)	(0.802)	(0.808)		

**denotes a significant correlation at the 0.01 level; * denotes a significant correlation at the 0.05 level

Table 7 Parameters of regression models (used in supplement Fig.1) of diffusive and ebullitive CH_4 fluxes as a function of water temperatures (*Tw*) at different concentrations of total phosphorous (*TP*).

Emissions ($mg·m^{-2}·h^{-1}$)	Averaged TP ($mg·L^{-1}$)	n	Tw			Ta		
			Q_{10}	p	R^2	Q_{10}	p	R^2
CH_4 diffusive	0.05	144	1.29	< 0.001	0.26	1.27	< 0.001	0.36
	0.1	96	1.79	< 0.001	0.46	1.62	< 0.001	0.58
	0.2	48	5.29	0.002	0.23	1.86	< 0.001	0.29
	0.4	144	7.52	< 0.001	0.69	5.23	< 0.001	0.43
	0.8	96	5.24	< 0.001	0.76	3.24	< 0.001	0.71
CH_4 ebullition	0.05	51	1.32	0.046	0.08	1.15	0.192	0.02
	0.1	52	1.85	0.211	0.04	1.27	0.407	0.02
	0.2	––	––	––	––	––	––	––
	0.4	––	––	––	––	––	––	––
	0.8	53	3.29	< 0.001	0.21	2.06	0.001	0.17

–– indicates that no exponential relationships were found

Figure Captions

Fig. 1 Diurnal and seasonal variability of the main environmental factors and CH_4 fluxes during the monitoring periods.

Fig. 2 Bin-averaged diffusive CH_4 flux (D_{CH4}) and the difference between water and air temperature ($\Delta T = Tw - Ta$). Symbols showed mean values within each temperature bin, error bars showed the respective standard deviation (SD represented the degree to which the data value deviates from the mean). The ellipse of the dotted line indicated D_{CH4} when ΔT was close zero.

Fig. 3 Changes of CH_4 ebullition (B_{CH4}, histograms) and frequency of daily CH_4 bubbling (grey area) versus the temperature difference between water and air (ΔT).

Fig. 4 (a) Daily total diffusive CH_4 flux (T_{DCH4}), and (b) daily total CH_4 ebullition (T_{BCH4}) as a function of mean daily water temperature ($\overline{Tw}$, black circles) and air temperature ($\overline{Ta}$, open circles). The solid lines represent the exponential relationships between pond fluxes and $\overline{Tw}$, the dashed lines represent the exponential relationships between pond fluxes and $\overline{Ta}$. The values of the temperature coefficient Q_{10} and the coefficients of determination (R^2) for the exponential fits are provided as labels in each graph.

Fig. 1 Diurnal and seasonal variability of the main environmental factors and CH_4 fluxes during the monitoring periods.

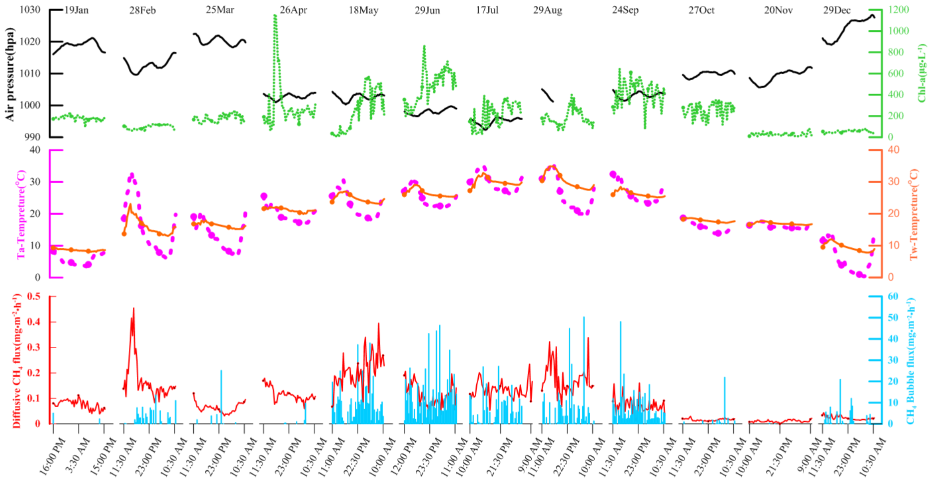

https://doi.org/10.5194/bg-2020-178
Preprint. Discussion started: 1 July 2020

Fig. 2 Bin-averaged diffusive CH_4 flux (D_{CH4}) and the difference between water and air temperature ($\Delta T = Tw - Ta$). Symbols showed mean values within each temperature bin, error bars showed the respective standard deviation (SD represented the degree to which the data value deviates from the mean). The ellipse of the dotted line indicated D_{CH4} when ΔT was close zero.

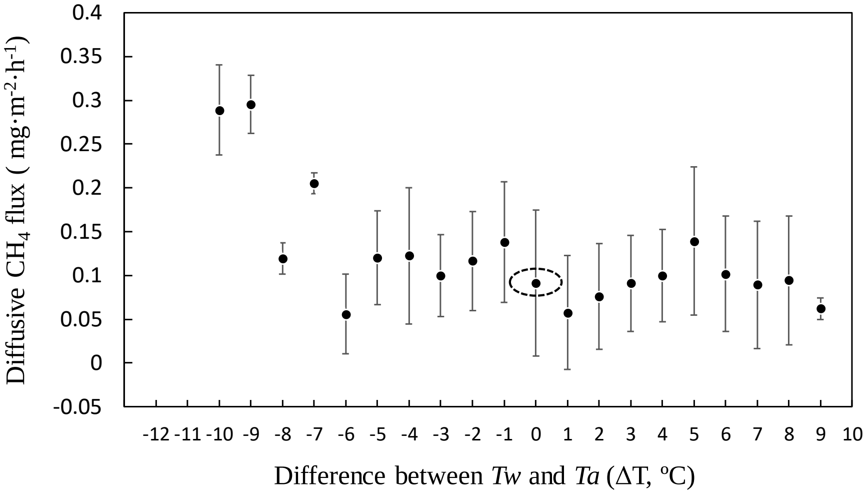

Fig. 3 Changes of CH_4 ebullition (B_{CH4}, histograms) and frequency of daily CH_4 bubbling (grey area) versus the temperature difference between water and air (Δ*T*).

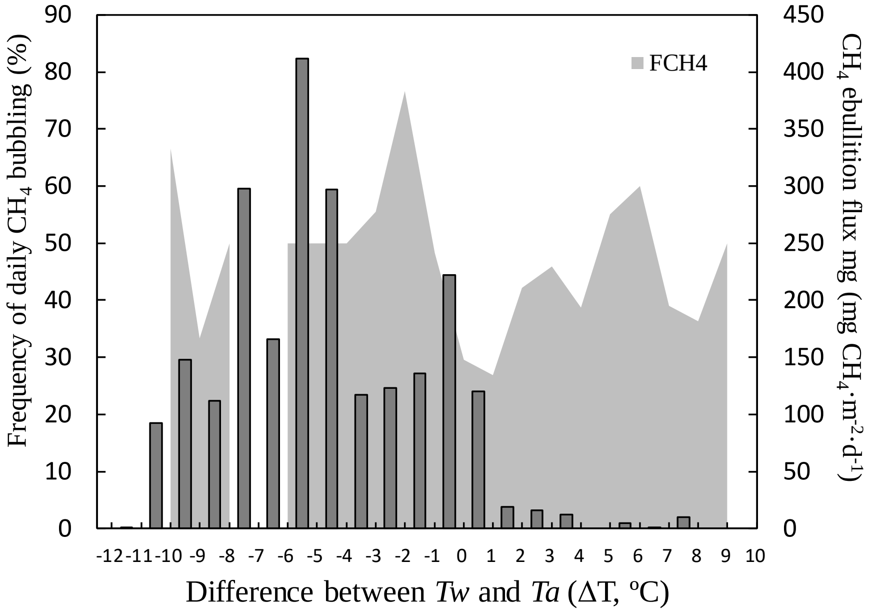

Fig. 4 (a) Daily total diffusive CH_4 flux (T_{DCH4}), and (b) daily total CH_4 ebullition (T_{BCH4}) as a function of mean daily water temperature ($\overline{Tw}$, black circles) and air temperature ($\overline{Ta}$, open circles). The solid lines represent the exponential relationships between pond fluxes and $\overline{Tw}$, the dashed lines represent the exponential relationships between pond fluxes and $\overline{Ta}$. The values of the temperature coefficient Q_{10} and the coefficients of determination (R^2) for the exponential fits are provided as labels in each graph.

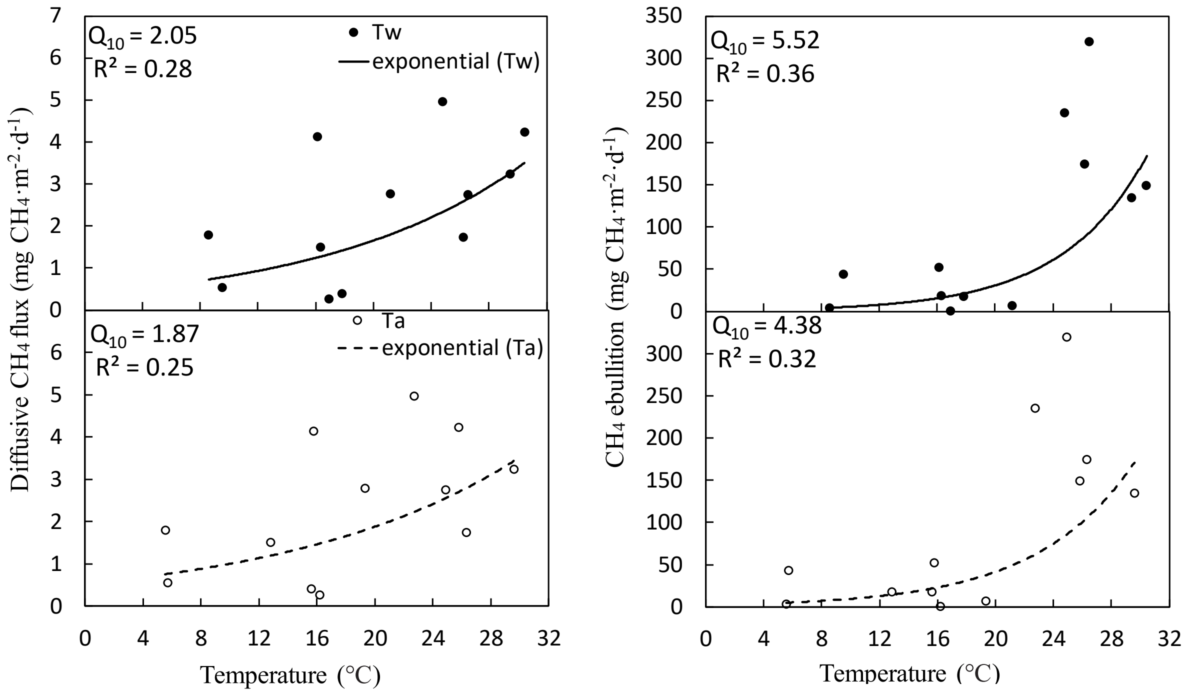

(a)

(b)